# Reconfigurable Digital Functionality of Composite Resonator Vertical Cavity Lasers

Kent D. Choquette, *Fellow, IEEE*, Chen Chen, *Student Member, IEEE*, Ann C. Lehman Harren, Daniel M. Grasso, and David V. Plant, *Fellow, IEEE*

(*Invited Paper*)

***Abstract*— The composite resonator vertical cavity surface laser can perform multiple digital functionalities at greater than 10 GHz bandwidth, including: direct intensity modulation, wavelength division multiplexing, multilevel pulse amplitude modulation, and optical picosecond pulse generation. The unique attributes of these microcavity lasers arise from the two strongly coupled optical cavities which can be electrically injected independently. Reconfiguration among multiple functionalities is achieved by control of the three terminal signals input into the laser and can be achieved using a high-speed digital circuit whose logic can be adjusted to provide appropriate modulation voltages to the optically coupled laser cavities. The novel optical properties of composite resonators are reviewed with a focus on several different digital functionalities possible from this semiconductor laser.**

***Index Terms*— High speed modulation, semiconductor lasers, vertical cavity surface emitting lasers.**

## I. Introduction

THE vertical-cavity surface-emitting laser (VCSEL) has become a dominant source for short-haul optical communications, mainly because of its low-cost high-volume manufacture, very low power consumption, and high-speed digital modulation. For emerging applications such as data center interconnects, access networks, and radio-over-fiber transmission, additional optical functionalities will be demanded from a VCSEL to further reduce the form factor and power consumption of future optical systems, as well as to scale up to 2-dimensional laser arrays. It will be beneficial if multiple functionalities from a microcavity laser can be rapidly reconfigured.

The integration of multiple functionality within an edge-emitting semiconductor laser structure, such as active and passive components, can be achieved by selective area epitaxy [1], [2] or via impurity induced intermixing [3]. For vertical cavity lasers, integration of functionality is limited by the practical consideration of the thickness of the required epitaxial materials. However because high quality factor optical cavities can be easily defined using semiconductor distributed Bragg reflector mirrors, stringently controlled optical coupling between two or more optical cavities can be achieved.

Recently composite resonator vertical cavity lasers (CRVCLs), first introduced by Stanley, *et al.* [4], have demonstrated a wide range of unique characteristics [5]–[21]. Leveraging these characteristics enables an equally diverse range of digital functionality, which may prove valuable for future optical interconnect sources. Reconfigurable functionality is possible in CRVCLs due to their unique ability to: (i) tailor the optical coupling between the monolithic cavities; (ii) dynamically modify the cavity interaction; and (iii) incorporate passive or active resonators. The composite resonators can be utilized to influence the spectral and temporal properties within a vertical microcavity laser. Using independent carrier injection into the cavities has facilitated demonstrations of several different analog and digital functionalities for optical communications [12]–[20].

We review the unique properties of composite resonator vertical cavity lasers as well as their multiple reconfigurable functionality. After first describing the basic laser structure and optical properties, we report the fabrication process which produces a three-terminal microcavity laser source. Next we present examples of the varied digital functionality that is possible, using a variety of different epitaxial designs (differing middle mirror period) and device structures (differing aperture sizes). We show 10 Gb/s large signal modulation and dual wavelength division multiplexing. Additionally, the CRVCL can be reconfigured to generate 10 Gb/s three- or four-level pulse amplitude modulation (PAM) signaling, or to produce an optical pulse train with a minimum pulse width of 34 ps, by applying digital modulation to both optical cavities simultaneously and adjusting the amplitude and phase difference between two modulation signals. These unique functionalities make the CRVCL attractive for future optical systems, especially when combined with a digital circuit whose logic can be reconfigured to apply appropriate modulation voltages to both optical cavities.

## II. Laser Structure and Fabrication

Fig. 1(a) shows a cross section sketch of the CRVCL and Fig. 1(b) shows a transmission electron micrograph of the

Manuscript received August 2, 2011; revised September 22, 2011; accepted September 24, 2011. Date of current version January 24, 2012.

K. D. Choquette is with the Department of Electrical and Computer Engineering, University of Illinois at Urbana-Champaign, Urbana, IL 61801 USA (e-mail: choquett@illinois.edu).

C. Chen is with Ciena Corporation, Ottawa, ON K2K 3C8, Canada (e-mail: chenchen@ciena.com).

A. C. L. Harren is with Sandia National Laboratories, Livermore, CA 94551 USA (e-mail: ann.harren@gmail.com).

D. M. Grasso is with Coherent, Inc., Santa Clara, CA 95054-1112 USA (e-mail: dan.grasso@gmail.com).

D. V. Plant is with the Department of Electrical and Computer Engineering, McGill University, Montreal, QC H3A 2A7, Canada (e-mail: david.plant@mcgill.ca).

Color versions of one or more of the figures in this paper are available online at http://ieeexplore.ieee.org.

Digital Object Identifier 10.1109/JQE.2011.2171328

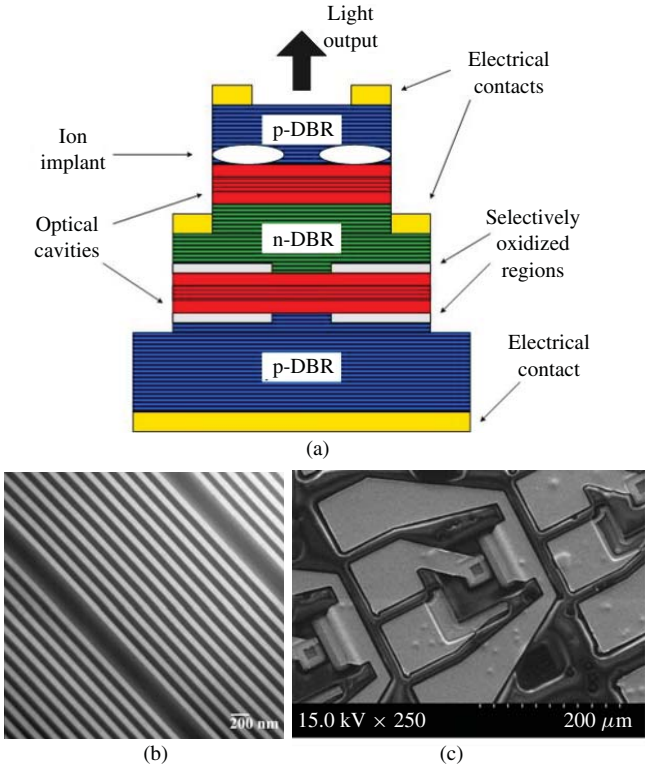


Fig. 1. Composite resonator VCSEL (a) side view sketch, (b) transmission electron micrograph cross section, and (c) scanning electron micrograph of fabricated laser with coplanar ground-signal-signal-ground high speed pads.

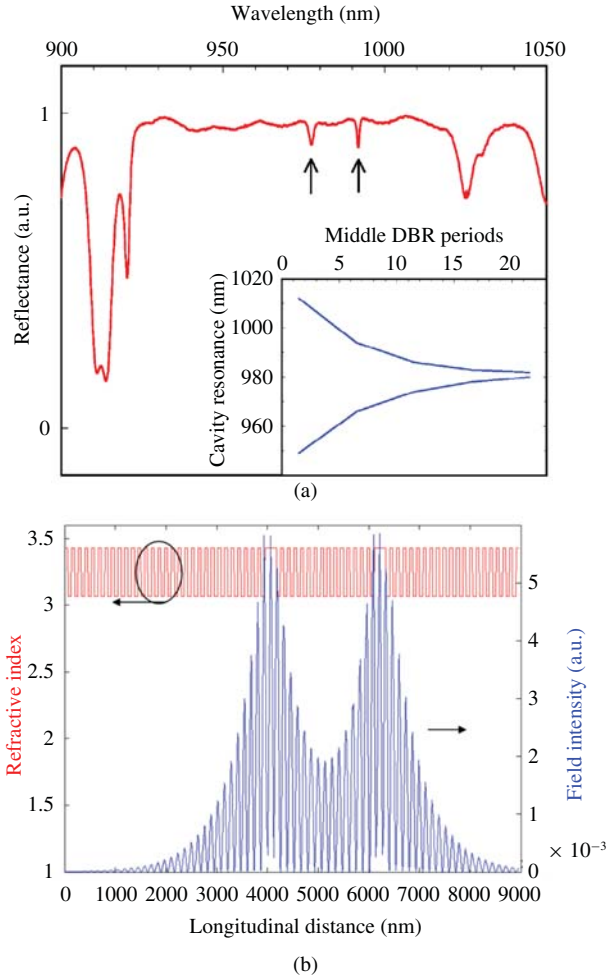


Fig. 2. (a) CRVCL reflectance spectrum showing two longitudinal modes (arrows), inset shows the resonance splitting versus middle mirror periods [7] and (b) sketch of refractive index and normalized optical field intensity for the short-wavelength longitudinal mode along the CRVCL growth direction.

epitaxial coupled cavities. The CRVCL epitaxial structure consists of a monolithic bottom p-type distributed Bragg reflector (DBR) with 35 periods, a middle n-type DBR with 5.5 to 15.5 periods, and an upper p-type DBR with 18 to 22 periods of $Al_{0.08}Ga_{0.92}As/Al_{0.92}Ga_{0.08}As$ layers. The middle DBR mirror separates two optical cavities as apparent in Fig. 1(b), each of which contains multiple GaAs quantum wells or InGaAs quantum wells for emission at nominally 850 or 980 nm, respectively. Note that the n-type middle mirror will function as the cathode of the two laser active regions. Both the top and bottom optical cavities have independent electrical contacts, which in Fig. 1(c) is accomplished with ground-signal-signal-ground coplanar contact pads [18]–[20].

The number of mirror periods of the middle DBR is the primary epitaxial design parameter. Fig. 2(a) shows the measured reflectance of a CRVCL structure with a 11.5 period middle mirror [7]. The coupling between the two cavities can be accurately controlled by changing the reflectance (number of DBR periods) of the middle DBR mirror. The inset of Fig. 2(a) shows the calculated cavity resonances as a function of periods in the middle DBR. The optical coupling of the cavity resonances is determined by the transmission of the shared middle DBR. A reduced number of middle mirror periods implies greater coupling between the cavities and thus larger spectral splitting; a resonance splitting between the two longitudinal modes as large as 30 nm is easily achievable. The optical modes extend into both cavities; a sketch of the intensity profile of one of the resonances is shown in Fig. 2(b). While the optical modes are distributed into both cavities, the carrier populations of the two cavities are relatively decoupled. In Fig. 2(b), we assume perfectly symmetric cavities; if the cavity lengths vary due to intentional (or unintentional) growth variation or differing current injection, then the mode profile will overlap one cavity more than the other [19].

The aperture sizes of the two optical cavities is the primary CRVCL device structure design parameter. To laterally define the CRVCL, we usually use a hybrid configuration. The top cavity is defined using ion implantation while the bottom cavity is defined using lateral oxidation. There have been a few reports using oxide confinement for both the top and bottom cavities [4], [12], [13], but our experience has found that this leads to differing and uncontrollable oxide aperture sizes. By using a top implant and bottom oxide aperture, a variety aperture size combinations can be designed. For example greater than 6 mW of single fundamental mode power has been demonstrated using a small top implant aperture with larger bottom oxide aperture [9]. Alternatively the highest direct modulation speed results from large top aperture with smaller bottom aperture [12], [20]. A disadvantage of this hybrid structure is the differing series resistance into each cavity, where the ion implanted cavity typically has higher resis-

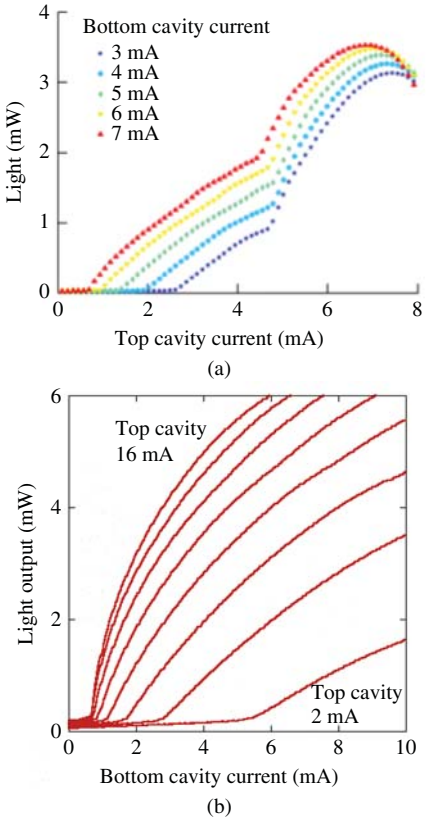


Fig. 3. (a) Light versus current into the top $8 \times 8$ $\mu$m$^2$ implant cavity with fixed current into the bottom $3 \times 3$ $\mu$m$^2$ oxide cavity of a CRVCL with 22/12.5/35 top/middle/bottom periods and (b) light versus current into the bottom $5 \times 5$ $\mu$m$^2$ oxide cavity with fixed current (steps of 2 mA) into the top $10 \times 10$ $\mu$m$^2$ oxide cavity of a CRVCL with 19/11.5/35 top/middle/bottom periods [13].

tance [22]. A concentric double mesa structure is fabricated as depicted in Fig. 1(a), with the smaller top mesa extending into the middle DBR, while the larger lower mesa extends into the bottom DBR. Ring electrical contacts are defined for the p-type contract on the top wafer surface, the n-type contact in the middle DBR, and another p-type contact in the bottom DBR or the substrate backside in order to have independent electrical injection into both cavities. The double mesa structure can be planarized using polyimide with top coplanar contacts on the polyimide surface as shown in Fig. 2(c) to reduce parasitic capacitance and facilitate high-speed signaling to both cavities [18]–[20].

## III. Laser Characteristics

Fig. 3 shows representative output light versus current curves at room-temperature with fixed current in one cavity while varying the current into the other for two different CRVCL wafers and device structures. Generally we find that the threshold current will decrease with increasing current injected into the other cavity; with sufficient current injected into one cavity, the apparent threshold can be reduced to zero [10]. For the laser of Fig. 3(a), the emission initially is the shorter wavelength longitudinal mode, and the kink observed in the output characteristics corresponds to the onset of lasing from the longer wavelength mode.

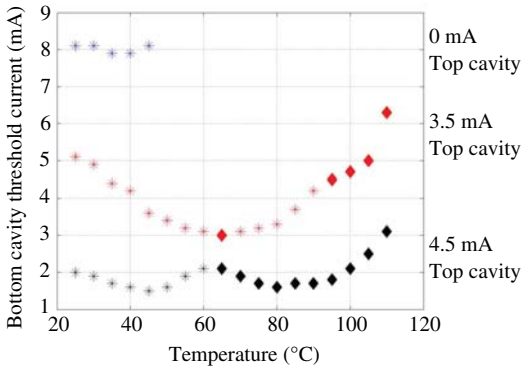


Fig. 4. Threshold current of the bottom cavity and dominant longitudinal mode for various biases on the top cavity of a CRVCL. For the upper/middle/bottom points, the top cavity current is 0/3.5/4.5 mA. An asterisk indicates that the short wavelength mode lases, and a diamond indicates that the long wavelength mode lases [11].

Note the slope efficiency can also vary, which is particularly pronounced for the device of Fig. 3(b). The CRVCL used in Fig. 3(b) has two square-shaped oxide apertures of $10 \times 10$ ($5 \times 5$) $\mu$m$^2$ size for the top (bottom) cavity. In Fig. 3(b), with 20 mA into the larger top cavity, the slope is approximately 6.35 W/A, which is greater than 400% differential quantum efficiency (at 850 nm) [13]. Above threshold, the slope decreases as the bottom cavity current is increased. The large slope efficiency and decrease in threshold current with increased upper cavity current persists under pulsed operation, and thus are not the result of thermal lensing effects, but rather are from the modification of optical loss.

The emission of a CRVCL is dependent on the spectral overlap between the resonances and the quantum well gain [10], [11]. Similar to a conventional VCSEL, changing the temperature causes the gain and cavity resonances to shift to longer wavelength, but at different rates. Therefore, the VCSEL threshold current will be approximately lowest at a temperature where the cavity resonance nears spectral alignment with the peak of the gain curve [22]. For temperatures higher and lower, the cavity resonance overlaps lower values of gain for the same injection current, and thus increased injection current (higher gain) is required to reach threshold, leading to a parabolic dependence of threshold current variation with temperature [23].

For the CRVCL, the threshold current temperature dependence (and emission spectrum) can be more complex. An example "double parabolic" threshold current temperature dependence (and threshold emission) for a CRVCL is shown in Fig. 4 [11]. Recall from Fig. 2 that because of the optical coupling between the cavities, there will be a long and short wavelength resonance. How these two longitudinal resonances spectrally overlap the quantum well gain will dictate not only the threshold gain, but also which resonance(s) will lase. For the CRVCL in Fig. 4, the short wavelength resonance operates at threshold; as the top cavity current and/or the ambient temperature increases, the long wavelength mode can reach threshold first and thus is the dominant threshold mode. Hence either the longer, shorter, or both resonances can lase in a CRVCL, depending on its design and bias. Although

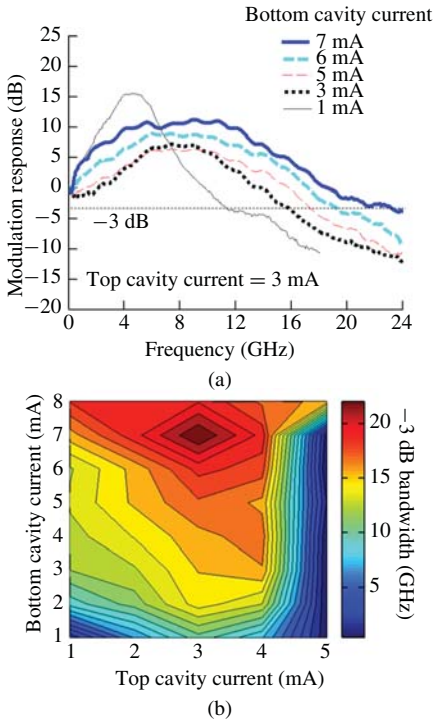


Fig. 5. Measured CRVCL small signal 3 dB response for (a) fixed top and varying bottom cavity current and (b) varying DC bias in both top and bottom cavities [20].

dual emission lasing has applications as shown below, it is usually advantageous to design the CRVCL to lase only on one (typically the longer wavelength) resonance.

## IV. Digital Laser Functionality

Unlike a conventional VCSEL, the photon population within a CRVCL is coupled to the carrier populations in both cavities simultaneously, but the carrier populations can be independently modified. The laser output of the CRVCL can be varied by applying independent dc bias to each of the cavities, as well as signal modulation to either or both of the coupled cavities, while varying the amplitude, phase, and frequency of the modulation signal(s) [12], [15]–[20]. In the following, we review a variety of digital functionality that can be demonstrated using a CRVCL, and show that reconfiguration between the functionalities can be relatively straightforward.

### A. Direct Digital Modulation

For high speed characterization, small-signal modulation characteristics of the CRVCL are measured using a network analyzer; large-signal modulation characteristics are obtained using a 25 GHz photodetector, a pattern generator and an oscilloscope. A cleaved 62.5/125 $\mu$m graded-index multimode fiber and a high speed photodetector are used to collect output light from the CRVCL under test. Fig. 5 shows small signal 3 dB bandwidth under modulation injection into the bottom cavity as a function of DC bias currents into the top and bottom cavity [20]. This particular CRVCL has 18 top/5.5 middle/35 bottom DBR mirror periods with a top $11 \times 11$ $\mu$m$^2$ implant aperture and bottom $5 \times 5$ $\mu$m$^2$ oxide

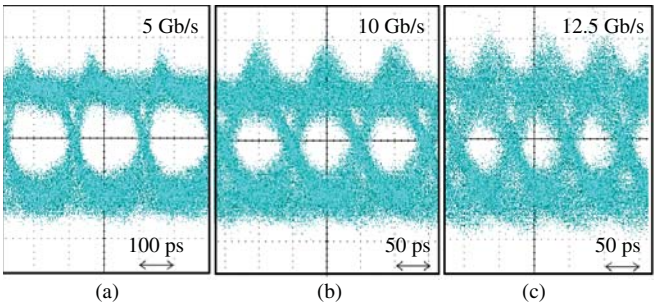


Fig. 6. Eye diagram of the CRCVL at a data rate of (a) 5 Gb/s, (b) 10 Gb/s, and (c) 12.5 Gb/s.

aperture. The maximum bandwidth achieved under direct modulation is 23 GHz as shown in Fig. 5(a). From Fig. 5(b) it is apparent that the bandwidth will depend the DC bias of both cavities. The small signal behavior can be analyzed using a rate equation model with two equations for each carrier population and one photon equation [20], [21]. In this analysis, the relative overlap of the mode with each cavity impacts the modulation bandwidth. As seen in Fig. 5(b), the change of the bottom cavity current leads to a more significant change in the modulation bandwidth than does the top cavity current, presumably due to its mode overlap with the bottom cavity.

Fig. 6 shows the large signal eye diagrams from a CRVCL with an $8 \times 8$ $\mu$m$^2$ implant and $4 \times 4$ $\mu$m$^2$ oxide aperture in the top and bottom cavities, respectively. The large signal modulation is shown in Fig. 6 at three different data rates for a back-to-back transmission, when direct modulation is applied to the top cavity only, and the dc current in the top and bottom cavity is 6 mA and 4 mA, respectively. A peak-peak modulation voltage of 2.5 V (the maximum voltage from the pattern generator) is used to open up the eyes in Fig. 6, due to the 760 ohm differential series resistance of the ion implanted top cavity. The extinction ratio is 3.2 dB for both the eyes at 5 Gb/s and 10 Gb/s. However, the degradation of the eye diagram becomes apparent when the CRVCL operates at 12.5 Gb/s. The largest $-3$ dB bandwidth is 8.5 GHz for this device, limiting the maximum data rate this particular CRVCL can support. Fig. 7 illustrates the bit error rate (BER) versus the received optical power for a back-back transmission. The lowest BER the CRVCL can achieve is $2.96 \times 10^{-9}$ and $1.27 \times 10^{-7}$ for the 5 Gb/s and 10 Gb/s operation, respectively.

### B. Wavelength Division Multiplexing

As mentioned previously, the CRVCL can lase on the short wavelength, long wavelength, or simultaneously both resonances by controlling the dc bias injected into the two optical cavities. This unique spectral behavior arises due to the effect of the spectral overlap between the resonances with the quantum well gain. As an example, Fig. 8 shows the CRVCL emission for four different combinations of input currents into the top and bottom cavities. Independent control of the dual lasing wavelengths provides the means to produce a two-channel wavelength division multiplexing source using a single laser which can be directly coupled to optical fiber. The four logic states in a two channel system (00, 01, 10, and 11) are thus rep-

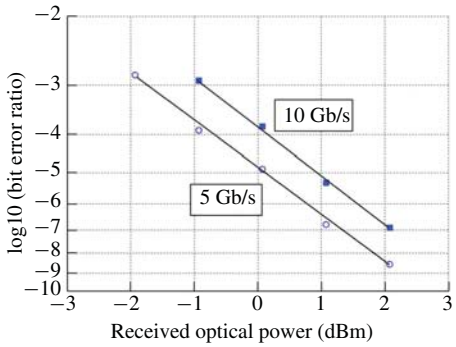


Fig. 7. Bit error rate versus received optical power at 5 Gb/s and 10 Gb/s for a back-to-back transmission.

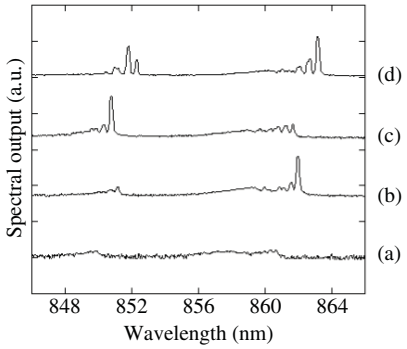


Fig. 8. CRVCL spectral output for the different logic states, top current (bottom current) = (a) 0.1 (0.1 mA), (b) 5.1 (0.1 mA), (c) 0.1 (6.1 mA), and (d) 5.1 (6.1 mA).

resented by Fig. 8(a), (b), (c) and (d), respectively. These currents have been selected such that a square wave modulation into both cavities, with one frequency twice the other, will produce all four spectral states shown in Fig. 8. This reduces the complexity of the current source, and would allow for independent data streams on each of the modulating current sources. Using early versions of lasers that lacked high speed coplanar contacts, we demonstrated an aggregate modulation speed of 20 MB/s [17]. In principle more channels could be added by increasing the number of coupled cavities, but would be accompanied by epitaxial and device fabrication complexity.

### *C. Alternative Modulation Schemes*

In addition to direct modulation using a single optical cavity, the CRVCL has the unique ability to manipulate its light output by modulating both optical cavities simultaneously [18]–[20]. Varying the phase and amplitude of dual modulation signals into the cavities provides some advantage for increased digital modulation rate, but at the cost of greater system complexity (e.g. two modulation sources). One exception may be the special case of injecting the same modulation signal, but 180° out of phase, into the top and bottom cavities. This modulation approach, which we call "push/pull" modulation, may enable high energy efficiency as well as significantly greater modulation speed [19].

Another advanced modulation scheme directly enabled by the CRVCL is pulse amplitude modulation (PAM). Injecting signals into both cavities produces an overall modulation

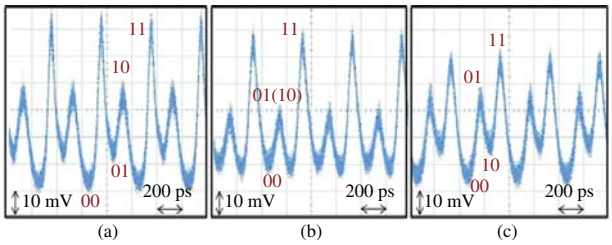


Fig. 9. 10 Gb/s PAM signaling when the modulation voltage in the top cavity is (a) 2.5 V, (b) 2.0 V, and (c) 1.7 V.

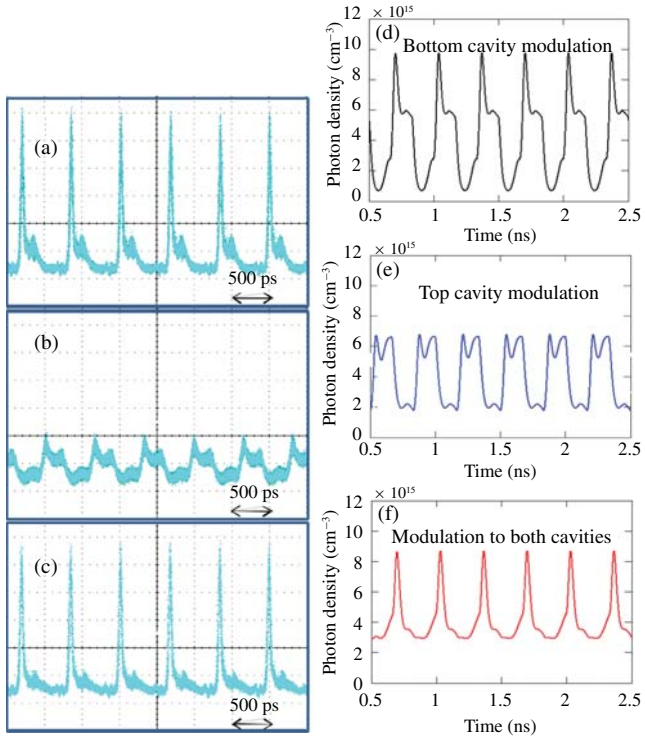


Fig. 10. Measured optical signal when digital modulation is applied to the (a) bottom cavity, (b) top cavity, and (c) both cavities. Simulated optical signal when digital modulation is applied to the (d) bottom cavity, (e) top cavity, and (f) both cavities.

response which is the summation of the modulation response from each individual cavity. This enables PAM-4 signaling by combining two binary signaling in the coupled cavities [18]. Using the same CRVCL device which exhibited the 10 Gb/s eyes (see Fig. 6), PAM signaling in shown in Fig. 9. This figure illustrates that the CRVCL generates two different patterns of PAM-4 signaling at 10 Gb/s, by only decreasing the modulation voltage in the top cavity from 2.5 V to 1.7 V, while maintaining the 2.5 V peak-to-peak modulation in the bottom cavity. Fig. 9(a) exhibits 4 amplitude levels, while in Fig. 5(b), two intermediate amplitude levels (i.e. level 10 and 01) coincide, producing the three-level PAM signaling. Note that the same dc biases are used in Fig. 9 as in Fig. 6.

### *D. Optical Pulse Generation*

Finally, the CRVCL under simultaneous digital modulation leads to a new approach to generate optical pulses. A conventional approach to produce optical pulses from a

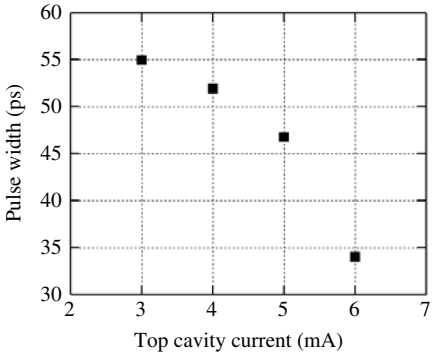


Fig. 11. Measured pulse width versus top cavity current of the CRVCL.

VCSEL is to apply a sinusoidal current modulation near the laser threshold [24], [25]. With the CRVCL, we find that the same digital circuit for the PAM signaling can be also used for generating optical pulses. Fig. 10 illustrates the pulse generation mechanism with the same CRVCL used in Figs. 6 and 9. When direct modulation is applied to the bottom cavity only, an extraordinarily large relaxation oscillation (RO) peak appears on the rising edge (see Fig. 10(a)). This large RO peak is related to the enhanced (or under-damped) modulation response at the RO frequency for small photon density in the laser cavity under low current injection [26], and may be also due to the cavity lifetime modulation associated with the current modulation [15]. In Fig. 10, the top and bottom cavity current for the CRVCL is 6 mA and 2 mA, respectively. Note that the bottom cavity is biased with a small dc current as compared to that in the PAM signaling case (Fig. 9), so that the large RO peak on the rising edge can be induced.

In order to form the optical pulse shown in Fig. 10(c), the large RO peak is extracted by simultaneously applying a nearly 180° out-of-phase modulation to the top cavity of the CRVCL, such that the optical signal following the RO peak is suppressed. In Fig. 10(c), the minimum pulse width and the repetition rate are 34 ps and 1.5 GHz, respectively. The pulse width becomes 28.7 ps after deconvolution.

The pulse generation can be modeled using a large signal CRVCL model in which the rate-equations are solved numerically in the time domain [19]. The cavity lifetime modulation can also be included in this calculation, and it would increase the amplitude of the generated pulses as expected [15], [20]. In Fig. 10(d)–(f) we illustrate the simulated pulse generation process, which is consistent with our experimental measurements. Fig. 11 shows the measured pulse width with different top cavity currents, while the bottom cavity current is fixed at 2 mA. The pulse width is inversely proportional to the dc current and thus the photon density, since the RO frequency is proportional to the square root of the photon density. The minimum pulse width of 34 ps is limited by the photon density in the CRVCL. The RF spectrum of the optical pulse is also measured, and is approximated by a Gaussian function.

## V. Conclusion

Future optical interconnect systems will demand additional new functionality from microcavity lasers, while maintaining the same high performance and low power operation that is expected from conventional VCSELs. We have reviewed the composite resonator vertical cavity laser which contains two optically coupled, but electrically independent cavities. The additional epitaxial and device structure complexity provides unique optical characteristics, which can be exploited for digital applications. We have shown that CRVCL can exhibit a small signal bandwidth greater than 20 GHz. The two optical resonances of the CRVCL can be utilized for dual wavelength division multiplexing into a single optical fiber. Finally, we have demonstrated that with the same digital circuit (e.g. the pattern generator in this work), the CRVCL can be configured to perform novel functionalities at several GHz. In particular, 10 Gb/s direct digital modulation, the generation of PAM-4 signaling, or short optical pulses are all demonstrated from the same device using the same digital circuit. The unique characteristics of CRVCL which enable multiple functionality makes the CRVCL a promising laser source for future optical systems where rapid reconfiguration among multiple optical functionalities is desired.

## Acknowledgment

The authors would like to thank A. Allerman and K. M. Geib at Sandia National Laboratories, Livermore, CA, for epitaxial wafers and technical discussions, Z. B. Tian at McGill University, Montreal, QC, Canada, for technical discussions on digital measurement, and J. J. Coleman for many technical discussions on semiconductor lasers.

## References

[1] Y. L. Wang, H. Temkin, R. A. Hamm, R. D. Yadvish, D. Ritter, L. H. Harriot, and M. B. Panish, "Semiconductor lasers fabricated by selective area epitaxy," *Electron. Lett.*, vol. 27, no. 15, pp. 1324–1325, Jul. 1991.

[2] T. M. Cockerill, D. V. Forbes, J. A. Dantzig, and J. J. Coleman, "Strained-layer InGaAs-GaAs-AlGaAs buried-heterostructure quantum-well lasers by three-step selective-area metalorganic chemical vapor deposition," *IEEE J. Quantum. Electron.*, vol. 30, no. 2, pp. 441–445, Feb. 1994.

[3] S. O'Brien and J. R. Shealy, "Monolithic integration on an (A1)GaAs laser and an intracavity electroabsorption modulator using selective partial interdiffusion," *Appl. Phys. Lett.*, vol. 58, no. 13, pp. 1363–1365, 1991.

[4] R. P. Stanley, R. Houdre, U. Oesterle, M. Ilegems, and C. Weisbuch, "Coupled semiconductor microcavities," *Appl. Phys. Lett.*, vol. 65, no. 16, pp. 2093–2095, Oct. 1994.

[5] P. Michler, M. Hilpert, and G. Reiner, "Dynamics of dual-wavelength emission from a coupled semiconductor microcavity laser," *Appl. Phys. Lett.*, vol. 70, no. 16, pp. 2073–2076, 1997.

[6] P. Pellandini, R. P. Stanley, R. Houdré, U. Oesterle, M. Ilegems, and C. Weisbuch, "Dual-wavelength laser emission from a coupled semiconductor microcavity," *Appl. Phys. Lett.*, vol. 71, no. 7, pp. 864–866, Aug. 1997.

[7] A. J. Fischer, K. D. Choquette, W. W. Chow, H. Q. Hou, and K. M. Geib, "Coupled-resonator vertical-cavity laser diode," *Appl. Phys. Lett.*, vol. 75, no. 19, pp. 3020–3022, 1999.

[8] A. J. Fischer, W. W. Chow, K. D. Choquette, A. A. Allerman, and K. M. Geib, "Q-Switched operation of coupled resonator vertical cavity laser diode," *Appl. Phys. Lett.*, vol. 76, no. 15, pp. 1975–1977, 2000.

[9] A. J. Fischer, K. D. Choquette, W. W. Chow, A. A. Allerman, D. K. Serkland, and K. M. Geib, "High single mode power observed from a coupled resonator vertical cavity laser diode," *Appl. Phys. Lett.*, vol. 79, no. 25, pp. 4079–4081, Dec. 2001.

[10] D. M. Grasso and K. D. Choquette, "Threshold characteristics of composite resonator vertical cavity lasers," *IEEE J. Quantum Electron.*, vol. 39, no. 12, pp. 1526–1530, Dec. 2003.

[11] A. C. Lehman and K. D. Choquette, "Threshold gain temperature dependence of composite resonator vertical cavity lasers," *IEEE J. Sel. Topics Quantum Electron.*, vol. 11, no. 5, pp. 962–967, Sep.–Oct. 2005.
[12] D. M. Grasso, D. K. Serkland, G. M. Peake, K. M. Geib, and K. D. Choquette, "Direct modulation characteristics of composite resonator vertical-cavity lasers," *IEEE J. Quantum Electron.*, vol. 42, no. 12, pp. 1248–1254, Dec. 2006.
[13] D. M. Grasso and K. D. Choquette, D. K. Serkland, G. M. Peak, and K. M. Geib, "High slope efficiency measured from a composite resonator vertical cavity laser," *IEEE Photon. Technol. Lett.*, vol. 18, no. 18, pp. 1019–1022, May 2006.
[14] J. V. Eisden, M. Yakimov, V. Tokranov, M. Varanasi, E. M. Mohammed, I. Young, and S. Ortyabrsky, "Optical decoupled loss modulation in a duo-cavity VCSEL," *IEEE Photon. Technol. Lett.*, vol. 20, no. 1, pp. 42–44, Jan. 2008.
[15] C. Chen, P. O. Leisher, D. M. Grasso, C. Long, and K. D. Choquette, "High-speed electroabsorption modulation of composite-resonator vertical-cavity lasers," *IET Optoelectron.*, vol. 3, no. 2, pp. 93–99, Apr. 2009.
[16] C. Chen and K. D. Choquette, "Microwave frequency conversion using a coupled-cavity surface emitting laser," *IEEE Photon. Technol. Lett.*, vol. 21, no. 19, pp. 1393–1395, Oct. 2009.
[17] E. W. Young, D. M. Grasso, A. Lehman, and K. D. Choquette, "Dual channel wavelength division multiplexing using a composite resonator vertical cavity laser," *IEEE Photon. Technol. Lett.*, vol. 16, no. 4, pp. 966–968, Apr. 2004.
[18] C. Chen and K. D. Choquette, "Multilevel amplitude modulation using a composite-resonator vertical-cavity laser," *IEEE Photon. Technol. Lett.*, vol. 15, no. 15, pp. 30–32, Aug. 2009.
[19] C. Chen, K. L. Johnson, M. Hibbs-Brenner, and K. D. Choquette, "Push-pull modulation of a composite-resonator vertical-cavity laser," *IEEE J. Quantum Electron.*, vol. 46, no. 4, pp. 438–446, Apr. 2010.
[20] C. Chen and K. D. Choquette, "Analog and digital functionalities of composite resonator vertical cavity lasers," *J. Lightw. Technol.*, vol. 28, no. 7, pp. 1003–1010, 2010.
[21] V. Badilita, J.-F. Carlin, M. Ilegems, and K. Panajotov, "Rate-equation model for coupled-cavity surface-emitting lasers," *IEEE J. Quantum Electron.*, vol. 40, no. 12, pp. 1646–1656, Dec. 2004.
[22] K. D. Choquette and K. M. Geib, "Fabrication and performance of vertical-cavity surface-emitting lasers," in *Vertical-Cavity Surface-Emitting Lasers*, C. Wilmsen, H. Temkin, and L. Coldren, Eds. Cambridge, U.K.: Cambridge Univ. Press, 1999.
[23] C. Chen, P. O. Leisher, A. A. Allerman, K. M. Geib, and K. D. Choquette, "Temperature analysis of threshold current in infrared vertical cavity surface emitting lasers," *IEEE J. Quantum Electron.*, vol. 42, no. 10, pp. 1078–1083, Oct. 2006.
[24] J. M. Wiesenfeld, G. Hasnain, J. S. Perino, J. D. Wynn, R. E. Leibenguth, Y.-H. Wang, and A. Y. Cho, "Gain-switched GaAs vertical-cavity surface-emitting lasers," *IEEE J. Quantum Electron.*, vol. 29, no. 6, pp. 1996–2005, Jun. 1993.
[25] M. Nakazawa, H. Hasegawa, and Y. Oikawa, "10-GHz 8.7 ps pulse generation from a single-mode gain-switched AlGaAs VCSEL at 850 nm," *IEEE Photon. Technol. Lett.*, vol. 19, no. 16, pp. 1251–1253, Aug. 2007.
[26] L. A. Coldren and S. W. Corzine, *Diode Lasers and Photonic Integrated Circuits*. New York: Wiley, 1995.

**Kent D. Choquette** (M'97–F'03) received the B.S. degree in engineering physics and applied mathematics from the University of Colorado-Boulder, Boulder, and the M.S. and Ph.D. degrees in materials science from the University of Wisconsin-Madison, Madison.

He held a post-doctoral appointment at AT&T Bell Laboratories, Murray Hill, NJ, from 1990 to 1992. He joined Sandia National Laboratories, Albuquerque, NM, from 1993 to 2000. He joined the University of Illinois at Urbana-Champaign, Urbana, in 2000, and is the Abel Bliss Professor in the Electrical and Computer Engineering Department, College of Engineering. He has authored more than 200 technical publications and three book chapters, and has presented numerous invited talks, and tutorials. His current research interests include design, fabrication, characterization, and application of vertical cavity surface-emitting lasers, photonic crystal light sources, nanofabrication technologies, and hybrid integration techniques for photonic devices.

Dr. Choquette has served as an Associate Editor of the IEEE JOURNAL OF QUANTUM ELECTRONICS, the IEEE PHOTONIC TECHNOLOGY LETTERS, and the *Journal of Lightwave Technology*, as well as a Guest Editor of the IEEE JOURNAL OF SELECTED TOPICS IN QUANTUM ELECTRONICS. He was awarded the IEEE/Photonic Society Engineering Achievement Award in 2008. He is a fellow of the Optical Society of America and the Society of Photographic Instrumentation Engineers.

**Chen Chen** (S'07) received the B.S., M.S., and Ph.D. degrees in electrical and computer engineering from the University of Illinois at Urbana-Champaign, Urbana, in 2004, 2006, and 2009, respectively.

He was a Post-Doctoral Fellow in electrical and computer engineering with McGill University, Montreal, QC, Canada, from 2009 to 2011. He is currently with Ciena Corporation, Ottawa, ON, Canada. He is the author/co-author of more than 50 journal and conference publications. His current research interests include semiconductor lasers and optoelectronics devices, optical interconnects, coherent optical transmission, and optical networking.

**Ann C. Lehman Harren** received the B.S., M.S., and Ph.D. degrees in electrical engineering from the University of Illinois at Urbana-Champaign, Urbana, in 2002, 2004, and 2007, respectively.

She is currently with Sandia National Laboratories, Livermore, CA. Her current research interests include laser diode arrays and novel detectors.

**Daniel M. Grasso** received the B.S. degree in electrical engineering and mathematics from the State University of NY-College-Buffalo, Buffalo, in 2000, and the M.S. and Ph.D. degrees from the University of Illinois at Urbana-Champaign, Urbana, in 2002 and 2006, respectively.

He is currently a Staff Optical Engineer with Coherent, Inc., Santa Clara, CA. His current research interests include high-power diode lasers, fiber lasers, and optical designs.

**David V. Plant** (S'85–M'89–SM'05–F'07) received the Ph.D. degree in electrical engineering from Brown University, Providence, RI, in 1989.

He was a Research Engineer with the Department of Electrical and Computer Engineering, University of California, Los Angeles, from 1989 to 1993. He has been a Professor and member with the Department of Electrical and Computer Engineering, Photonic Systems Group, McGill University, Montreal, QC, Canada, since 1993, and the Chair of the Department from 2006 to 2011. He is the Director and Principal Investigator of the Center for Advanced Systems and Technologies Communications, McGill University. He is a James McGill Professor and an IEEE Lasers and Electro-Optics Society Distinguished Lecturer. From 2000 to 2001, he took a leave of absence from McGill University to become the Director of the Optical Integration, Accelight Networks, Pittsburgh, PA. His current research interests include optoelectronic very large scale integration, analog circuits for communication, electro-optic switching devices, and optical network design including optical code-division multiple access, radio-over-fiber, and agile packet switched networks.

Dr. Plant has received five teaching awards from McGill University, including most recently the Principal's Prize for Teaching Excellence in 2006. He was a recipient of the R. A. Fessenden Medal and the Outstanding Educator Award, both from IEEE Canada, and received the NSERC Synergy Award for Innovation. He is a member of Sigma Xi and a fellow of the Optical Society of America.